SUPPORTING MATERIALS AND METHODS

***Reagents*.** ATRA (*all trans* retinoic acid), AM580, cholesterol, insulin, oleate, retinyl palmitate, and cycloheximide were from Sigma Aldrich. ATRA and AM580 are selective RAR agonists. Lipopolysaccharide (LPS) was from Enzo. GW3965 and GW7845 were gifts from P. Tontonoz. GW3965 is a specific LXR agonist and GW7845 is a specific PPARg agonist in nanomolar concentrations. Cholesterol intermediates were obtained from Steraloids. In cell culture experiments, treatments were applied for 12-14 hours. Treatments were performed on day 2 of culture activation of HSCs. For treatments with nuclear receptor agonists, cells were cultured in 2% charcoal stripped serum (LPDS, Gibco) overnight prior to reagent addition. Cycloheximide pre-treatment was for one hour prior to adding other reagents.

Cell Culture, siRNA Transfections, Lipid Loading, Oil Red O Staining and Immunohistochemistry. Primary HSCs were cultured on poly-d-lysine coated dishes in DMEM (100 mg/dL glucose), 15% fetal bovine serum (FBS), 1% pen/strep and 1% amphotericin (GIBCO). Human LX-2 cells were a gift from S. Friedman and cultured on uncoated plastic in DMEM (100 mg/dL glucose) + 10% FBS + 1 % pen/strep. The 3T3-L1 and 10T1/2 cells were differentiated into adipocytes as previously described using the PPARg agonist GW7845 (as per Park et al, *J Lipid Research*, 51:2775-84, 2010). *Rab18* knockdown was performed by transfecting primary stellate cells using FuGene (Roche) in complex with a specific *Rab18* siRNA oligonucleotide or scrambled control (Invitrogen). Lipid loading in LX-2 cells was performed with an emulsion of varying amounts of oleate, retinyl palmitate, and 2% BSA as carrier for 24 hours prior to experiments. Oil red O (ORO) staining was carried out by standard protocol using 5% ORO stock solution diluted and strained further in PBS. Cells were fixed in 10% formalin and imaged at 4X magnification.

Rab18 Mutagenesis. Mouse and human wild type Rab18 expression clones in pCMV-AC6 were purchased from Origene. Mutations (Q67L, S22N and C203A) were made by site-directed mutagenesis kit (Stratagene). Q67L has constitutively active GTPase activity, S22N has constitutively inactive GTPase as it preferentially binds GDP, and the C203A mutant stops the insertion of Rab18 into membranes by its inability to be isoprenylated. Primer sequences for mutagenesis available upon request. Transient transfections of primary HSCs and LX-2s using Fugene (Promega) were performed according to manufacturer's protocol.

Immunoblot and Immunohistochemistry Analysis. Cytoplasmic and membrane proteins were extracted from cells or whole tissue using specific buffers containing 0.5% IGEPAL. Membrane fraction proteins were extracted using a Mem-Per assay kit (Thermoscientific) and optimized using sodium deoxycholate to extract hydrophobic proteins. Protein concentrations were determined by the Bradford assay (BioRad). 10-50 mg of denatured protein was separated by SDS-PAGE using the NuPage system (Invitrogen). Protein was transferred to PVDF membranes, which were then blocked with 5% BSA in TBS-1% Tween. Membrane were incubated with 1° antibodies overnight (1:1000), washed, and then incubated with 2° HRP-conjugated antibody (1:2000) for one hour at room temperature. Bands were detected using the ECL system (Amersham). Primary antibodies were as follows: *Rab18* (Abcam); *Na^+-K^+-ATPase* (Cell Signaling Technology); *Plin3* (*Tip47*), *Gapdh* and b-*Actin* (Santa Cruz). Band density was quantified using the histogram function to count pixels on Photoshop (Adobe).

For immunohistochemistry, primary or immortalized cells were seeded for 24 hours at 60% confluence on 8-well Transwell slides (Thermo Scientific). After treatments, cells were washed with PBS, fixed in 10% formalin for 30 minutes, washed in PBS, permeabilized in 0.1% Triton in PBS, and washed again with PBS before staining. To ensure specificity of our stainings,

additional experiments were performed where cells were fixed for 20 minutes in 4% paraformaldehyde, and permeabilized in 0.1 mg/mL saponin and blocked with 5% BSA. A 45 minute incubation with 0.2M glycine blocked was performed to quench background fluorescence from aldehydes. 1° antibodies were used at the following dilutions: *Acta2* 1:500. Reagents for staining neutral lipid (BODIPY) (Molecular Probes) and nuclei (DAPI) (Molecular Probes) were used at 1:1000 and 1:10000, respectively. For *Rab18* staining, fixed cells were blocked with 5% BSA in PBS for 1 hour, incubated with *Rab18* primary antibody (1:100, rabbit polyclonal; Abcam, Ab119900), washed with PBS, and then incubated with a secondary goat anti-rabbit antibody (1:1000, dylight 350 conjugate; Fisher). Cells were imaged on a Zeiss Z1 AxioObserver fluorescent microscope.

***Microarray Analysis*.** Gene ontology and expression data were analyzed and clustered using GeneSpring GX (version 12.5, Agilent Technologies). The data (probe set) values were normalized to 5 housekeepers (*18S, b-Actin, Gapdh*, *PyruCarb* and *TransRec*). After normalization, the data was log transformed in order to obtain fold increase or decreases (cutoff ^{3} 2x change). Day-wise paired comparisons between each genotype were analyzed with Pearson's correlation. Hierarchical tree clustering (tree or K-means clustering) was carried out to show temporal relationships across the days of culturing for each genotype. The online bioinformatics resource DAVID (http://david.abcc.ncifcrf.gov) was used for gene ontology analysis.

Lipid Analysis and Mass Spectroscopy. Solvents were from Fisher Scientific. All samples were harvested in low-light / dark conditions and flash-frozen in liquid N_2 (tissues) or stored immediately at -80^{o}C (cell pellets) prior to analysis. Tissues were homogenized in 10 volumes

of PBS using a Polytron homogenizer (Brinkmann Instruments) set at half maximal speed for 10 s. Pelleted cells were resuspended in 1.0 ml of PBS and similarly homogenized using a Polytron homogenizer. Equal volumes of absolute ethanol containing a known amount of retinyl acetate as an internal standard were added to aliquots of samples, and the retinoids extracted into hexane. After one backwash against doubly distilled H_2O, the hexane extract was evaporated to dryness under a gentle stream of N_2. The retinoid containing film was dissolved in 40 mL of benzene for injection onto 4.6 X 250 mm Ultrasphere C_{18} HPLC columns (Beckmann, Fullerton) preceded by a C_{18} guard column (Supelco) using 70% acetonitrile-15% methanol-15% methylene chloride as the running solvent flowing at 1.8 ml/min. Retinol and retinyl esters (retinyl palmitate, oleate, linoleate, and stearate) were detected at 325 nm and identified by comparing the retention times and spectral data of experimental compounds with those of authentic standards. Concentrations of retinol and retinyl esters in the tissues were quantitated by comparing integrated peak areas for those of each retinoid against those of known amounts of purified standards. Loss during extraction was accounted for by adjusting for the recovery of internal standard added immediately after homogenization of the samples. The samples were plotted as µg retinoid per million cells.

For oxysterol mass spectroscopy, all solvents were from Fisher Scientific. Cholesterol and oxysterol standards were from Steraloids, while a heptadeuterated-cholesterol (chol-d7) internal standard was from Avanti Polar Lipid. Stellate cells were isolated from WT and *Lxra*b$^{-/-}$ mice and flash frozen in liquid N_2. Briefly, 3 ml of chloroform:methanol (v:v = 2:1) containing 50 pmol of chol-d7 as internal standard was added to 100 ml of sample homogenate in a clean glass tube and vortexed thoroughly. 500 ml of PBS was then added to allow for phase separation. The mixture was vortexed again and centrifuged at 3,000 x *g* for 10 minutes. The lower organic phase was transferred to a second clean glass tube using a Pasteur pipette. 2 mL of chloroform

was added to the residual aqueous phase, followed by vortex mixing and centrifugation again at 3,000 x *g* for 10 minutes, to extract any remaining lipids. The two organic phases were pooled and evaporated under nitrogen. The extracted lipids were reconstituted in 50 ml of methanol and transferred to LC/MS/MS autosampler vials (Waters) for injection. Mass spectroscopy was carried out on a Waters Xevo TQ MS ACQUITY UPLC system (Waters), controlled by Mass Lynx Software version 4.1. Samples were maintained at 4°C in the autosampler and 5 ml loaded onto a Waters ACQUITY UPLC BEH Phenyl column (3 mm inner diameter × 100 mm with 1.7 µM particles), preceded by a 2.1 × 5 mm guard column containing the same packing materials. The column was maintained at 40 °C throughout analysis. The UPLC flow rate was continuously 300 ml/min in a binary gradient mode with the following mobile phase as described previously with modification: initial flow conditions were 15% solvent A (water, containing 0.2% formic acid and 1 mM ammonium formate) and 85% solvent B (methanol, containing 0.2% formic acid and 1 mM ammonium formate). Solvent B was increased linearly to 99% over a 10 min period. Then the column was conditioned using the initial gradient for 2 minutes before the next injection. Steroids of interest eluted between 2.5 and 7.5 min. Positive ESI-MS/MS mass spectrometry with multiple reaction monitoring (MRM) mode was performed using the following parameters: capillary voltage, 3.8 kV; source temperature, 150°C; desolvation temperature, 500°C; desolvation gas flow, 1000 L/hr; and collision gas flow, 0.15 mL/min. The optimized cone voltage was 22 V, collision energy for multiple reactions monitoring mode (MRM) was 26 eV. Different species were identified by comparing the retention times of experimental compounds with those of authentic standards. Concentrations of steroids in the samples were quantitated by comparing integrated peak areas for those against those of known amounts of purified standards. Loss during extraction was accounted for by adjusting for the recovery of the internal standard added before extraction. The samples were plotted as pmol/mg DNA.

Cellular cholesterol and cholesterol esters were measured using a colorimetric kit (Biovision). Cells were homogenized and spun at 15,000 x *g* for 10 minutes. Cholesterol was extracted using a chloroform:isopropanol:NP40 (7:11:0.1) mixture. The organic phase was removed to a new tube and air dried at 50˚C to remove chloroform. Samples were dried under vacuum for 30 minutes. Dried cholesterol was resuspended in 100 µl of the assay buffer. The cholesterol assay was carried according to the manufacturer's instructions: sample aliquots are combined with buffer, cholesterol probe, assay enzyme mix and incubated with or without esterase. The presence of a cholesterol oxidase causes oxidation of cholesterol at 37˚C to yield H_2O_2, which reacts with the cholesterol probe and is measured in a spectrophotometer at 570nm. In the presence of the esterase, the assay detects total cholesterol in the presence of the esterase and free cholesterol in its absence. Cholesterol ester content is measured as the difference between cellular cholesterol and free cholesterol. Values were obtained using a cholesterol standard curve and plotted as mg per million cells.

ACKNOWLEDGEMENT: We thank Peter Tontonoz for LXR null mice, the GW3965 and GW7845 compounds and helpful insights on the manuscript; Scott Friedman for helpful insights on the manuscript; Brad Jones for a generous gift in support of our laboratory.

SUPPLEMENTARY FIGURE LEGENDS

Supplementary Figure 1. Array analysis and gene ontology between WT and LXR null hepatic stellate cells. Purified, primary stellate cells from WT and *Lxr*ab$^{-/-}$ mice were allowed to culture activate on plastic for 1, 2, 3 and 5 days. **(A)** Venn diagrams show numbers of shared or unique genes from each genotype. Increases in gene expression are shown in red, decreases in blue. **(B)** Gene ontology (GO) analysis summary of changed biological functions in cells from days 2 and 3 of culture. In general, there are more gene changes in *Lxr*ab$^{-/-}$ cells compared to WT. Minimal level of detection is 2x change (red = increase, blue = decrease).

Supplementary Figure 2. Gene expression in freshly isolated stellate cells. Basal levels of gene expression in primary stellate cells from WT and *Lxr*ab$^{-/-}$ mice are shown to demonstrate no significant differences in genes related to fibrosis **(A)** or retinoic acid signaling **(B)**. As expected, *Lxr*ab$^{-/-}$ cells have marked differences in inflammatory **(C)** and LXR target gene expression **(D)**. All data are mean ± SEM, analyzed by t-tests. *, $P < .05$; NS, $P > .05$.

Supplementary Figure 3. Validation of targets from gene array analysis. Quantitative validation (qRT-PCR) of changes during primary stellate cell culture activation for fibrotic genes *Acta2* **(A)** and *Col1a1* **(B)**, the LXR target gene, *Scd1*, **(C)** and inflammatory *Il-6* **(D).** These examples confirm the findings in the heat map of Figure 2. All data are mean ± SEM, analyzed by 1-way ANOVA with post-hoc tests. *, $P < .05$; **, $P < .01$; ***, $P < .001$; NS, $P > .05$.

Supplementary Figure 4. Characterization of retinoid responses in hepatic stellate cells. Purified, primary stellate cells from WT and *Lxr*ab$^{-/-}$ mice were cultured for 48 hours before

treatments. **(A,B)** HSCs were treated with ATRA (100 nM) and AM580 (100 nM) to examine modulation of RAR target genes (*Aldh1a1*, *Rbpr2* and *Crbp1*) by qRT-PCR. **(C)** Gene expression of a selected target, *Crbp1*, by qRT-PCR in response to dose escalation of ATRA is shown. **D)** RAR isoform expression (N=12 mice/genotype) and response to RAR agonists on day 2 (N=3-5 mice per genotype). Fold changes are mean ± SEM and differences between multiple groups compared by 1-way ANOVA with *post-hoc* tests: *, P < .05; **, P < .01; ***, P < .001, NS, P > .05.

Supplementary Figure 5. Characterization of perilipin expression profile in hepatic stellate cells. **(A)** HSCs from WT and *Lxr*ab$^{-/-}$ mice were screened for perilipin isoform expression on day 0 of culture activation, when lipid droplet content was still high, against white adipose tissue (WAT) and differentiated adipocyte cell lines (10T1/2 and 3T3-L1). HSCs primarily express *Plin2* and *Plin3.* *Plin1 and Plin5* are increased in WAT. Gene expression by qRT-PCR is shown. **(B)** No significant changes in *Plin2* expression occur in either *Lxr*ab$^{-/-}$ or WT primary stellate cells activating on plastic, even though both genotypes robustly express it. But *Plin3* expression (qRT-PCR) is basally higher and diminishes rapidly in activating *Lxr*ab$^{-/-}$ stellate cells. N=12 mice per genotype. **(C)** Immunoblotting shows loss of *Plin2* and *Plin3* in both WT and *Lxr*ab$^{-/-}$ HSCs; *Plin3* is the predominant perilipin in both genotypes. N=3-5 mice per genotype. **(D)** Immunoblotting shows redistribution of *Plin3* protein from membrane-bound to cytosolic fractions in *Lxr*ab$^{-/-}$ HSCs between day 1 and 3 of culture activation. Positive control to demonstrate correct fractionation of the samples is shown at right. All data are mean ± SEM, analyzed by 1-way ANOVA with post-hoc tests **(B)** or two-tailed t-tests **(C,D)**. *, P < .05; **, P < .01; ***, P < .001.

Supplementary Figure 6. Rab18 and perilipin immunofluorescent microscopy in stellate cells. (A) In paraformaldehyde-fixed *Lxra*b$^{-/-}$ HSCs on day 3 of culture activation, endogenous Rab18 (red) coats only the largest remaining auto-fluorescent lipid droplets. This staining is identical to that of endogenous Plin3 from the same experiment. **(B)** Under 63x magnification, Plin3 phenocopies the immunofluorescent staining of Rab18 in *Lxra*b$^{-/-}$ HSCs on day 3 of culture activation (cf. Fig. 4B), while Plin2 is concentrated at the perimeter of lipid droplets.

Supplementary Figure 7. Primary stellate cell responses to LPS, RAR/LXR agonists, and endogenous oxysterols. *Rab18* mRNA expression in day 2 culture activated primary WT and *Lxra*b$^{-/-}$ HSCs treated with **(A)** LPS (1 ng/mL), ATRA (100 nM), AM580 (100 nM), GW3965 (1 mM), or **(B)** endogenous oxysterols (100 mg/mL). Also shown is qPCR confirmation of equivalent transfection of WT and mutant Rab18 constructs in **(C)** experiments from primary WT stellate cells shown in Figure 5F and **(D)** experiments of LX-2 stellate cells shown in Figure 6E. All data are mean ± SEM, analyzed by 1-way ANOVA with post-hoc tests. *, $P < .05$; **, $P < .01$; ***, $P < .001$; N.S. $> .05$.

Supplementary Figure 8. Knockdown of Rab18 blocks primary stellate cell activation. (A) *Rab18* siRNA knockdown in *Lxra*b$^{-/-}$ HSCs on day 3 of culture activation results in ~50% in Rab18 mRNA. **(B)** The knockdown does not affect the expression of inflammatory markers *IL6* or *Ccl2*. But *Rab18* knockdown specifically diminishes the expression of canonical stellate cell activation markers related to **(C)** cytoskeletal changes (*Desmin*), **(D-F)** extracellular matrix remodeling (*Mmp2, Timp1, Timp2*), and autocrine driven stellate cell proliferation (*Pdgfr*). All data are mean ± SEM, analyzed by 1-way ANOVA with post-hoc tests: ***, $P < .001$; N.S. $> .05$.

A

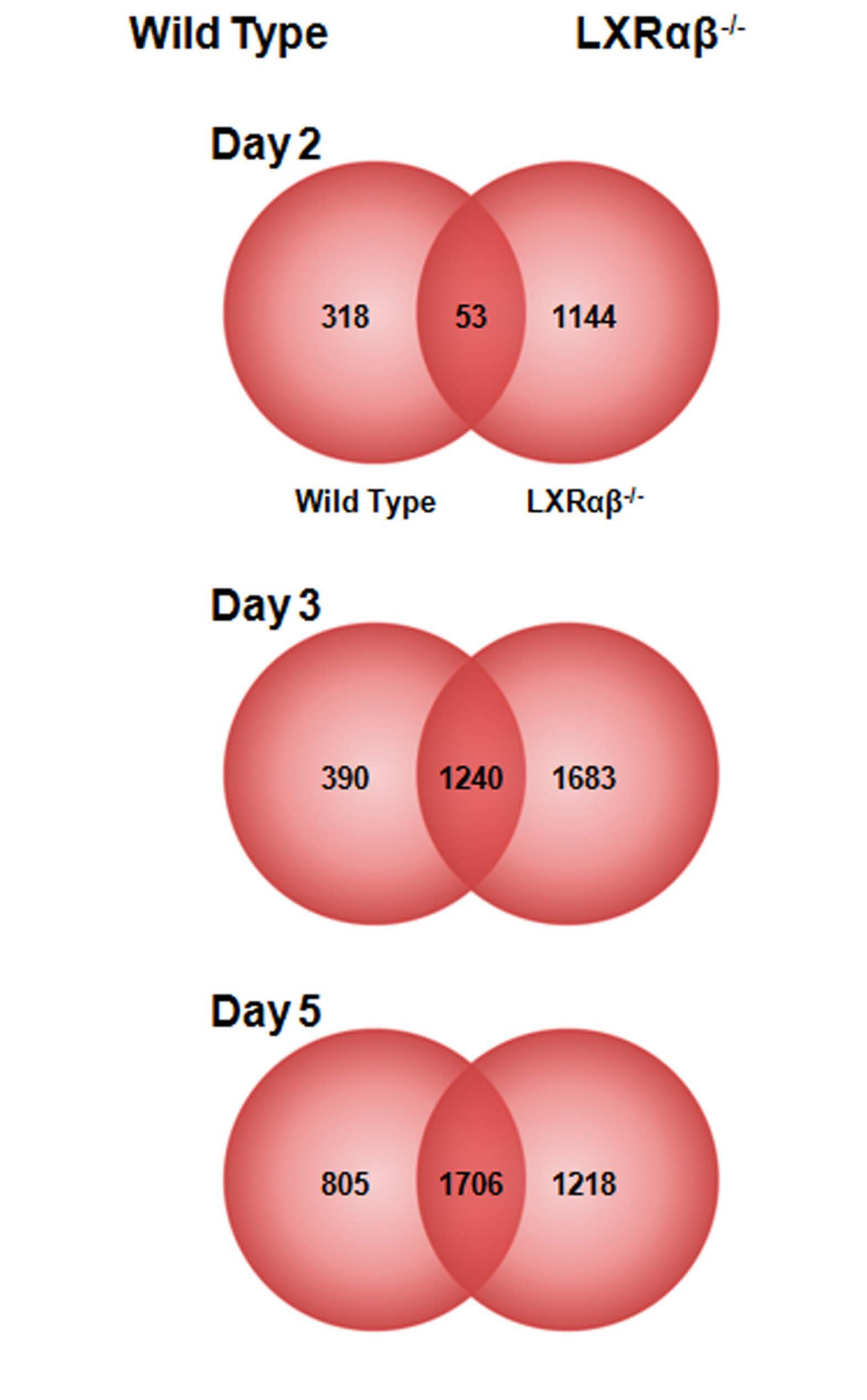
Wild Type
LXRαβ-/-
Day 2
318
53
1144
Wild Type
LXRαβ-/-
Day 3
390
1240
1683
Day 5
805
1706
1218
Increase

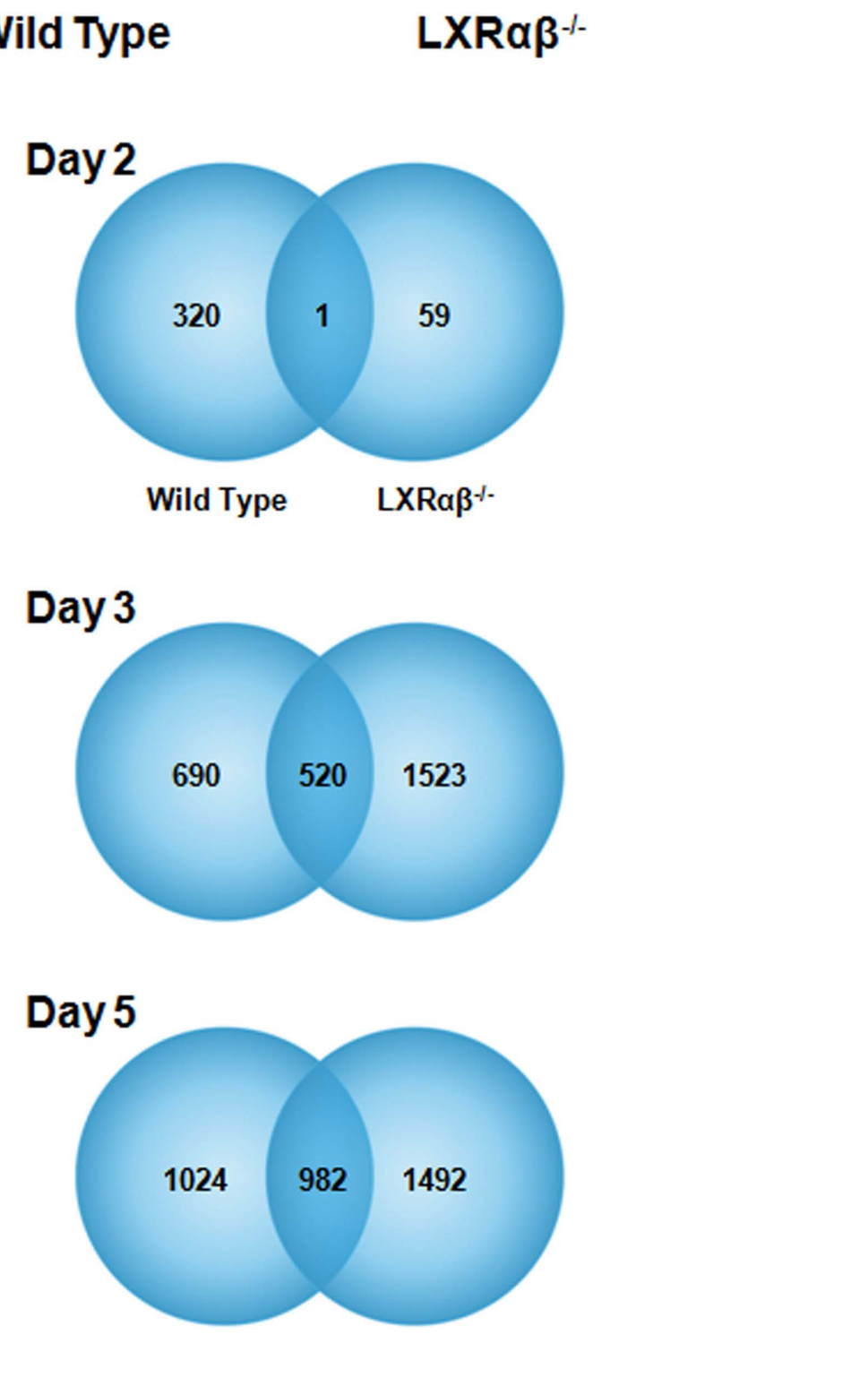
Wild Type
LXRαβ-/-
Day 2
320
1
59
Wild Type
LXRαβ-/-
Day 3
690
520
1523
Day 5
1024
982
1492
Decrease

B

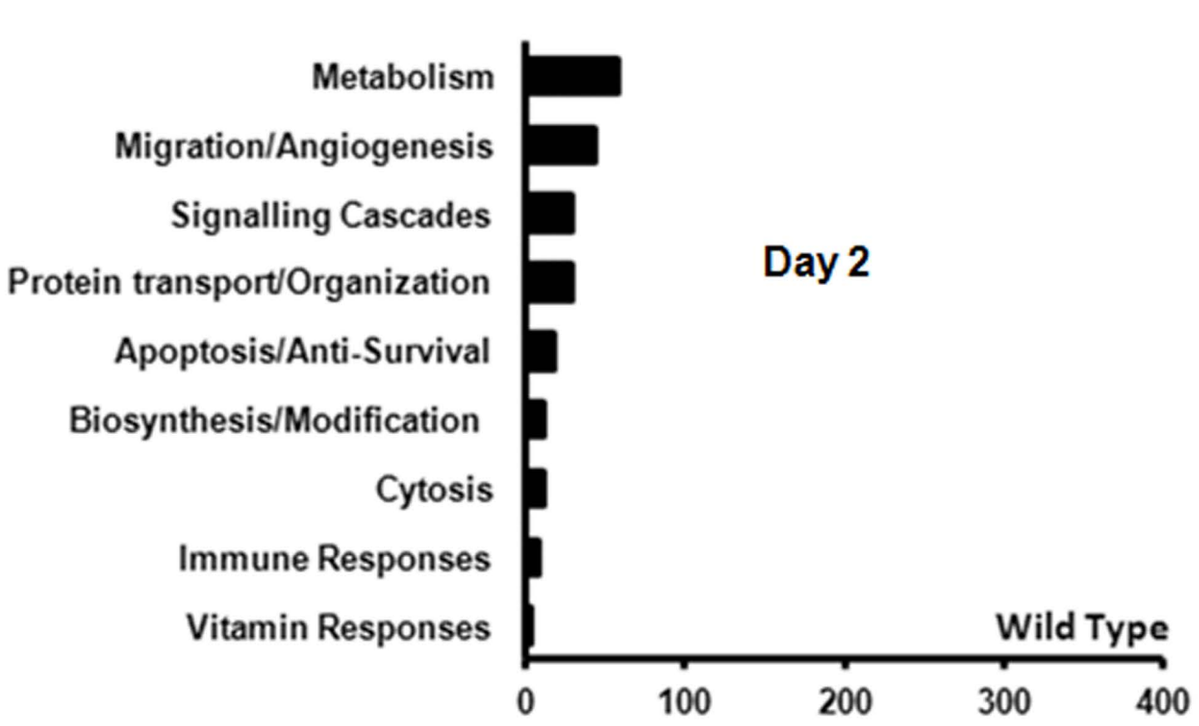
Metabolism
Migration/Angiogenesis
Signalling Cascades
Protein transport/Organization
Apoptosis/Anti-Survival
Biosynthesis/Modification
Cytosis
Immune Responses
Vitamin Responses
Day 2
Wild Type
0
100
200
300
400

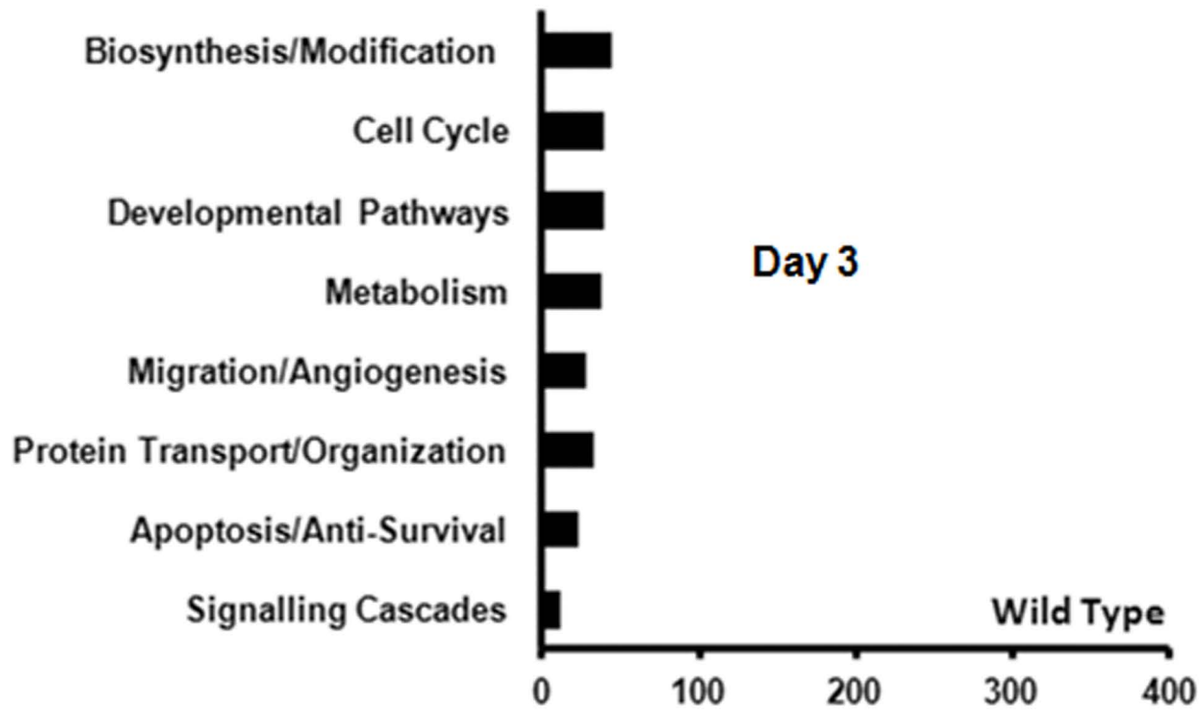
Biosynthesis/Modification
Cell Cycle
Developmental Pathways
Metabolism
Migration/Angiogenesis
Protein Transport/Organization
Apoptosis/Anti-Survival
Signalling Cascades
Day 3
Wild Type
0
100
200
300
400

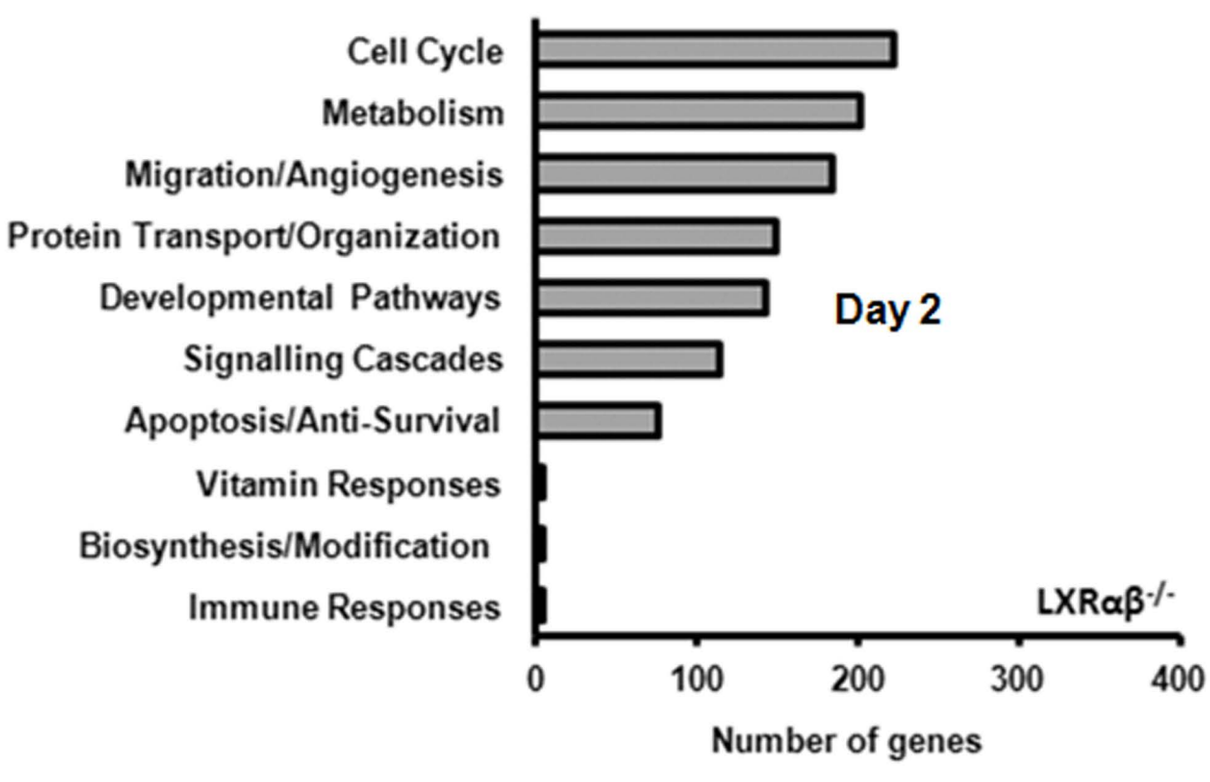
Cell Cycle
Metabolism
Migration/Angiogenesis
Protein Transport/Organization
Developmental Pathways
Signalling Cascades
Apoptosis/Anti-Survival
Vitamin Responses
Biosynthesis/Modification
Immune Responses
Day 2
LXRαβ-/-
0
100
200
300
400
Number of genes

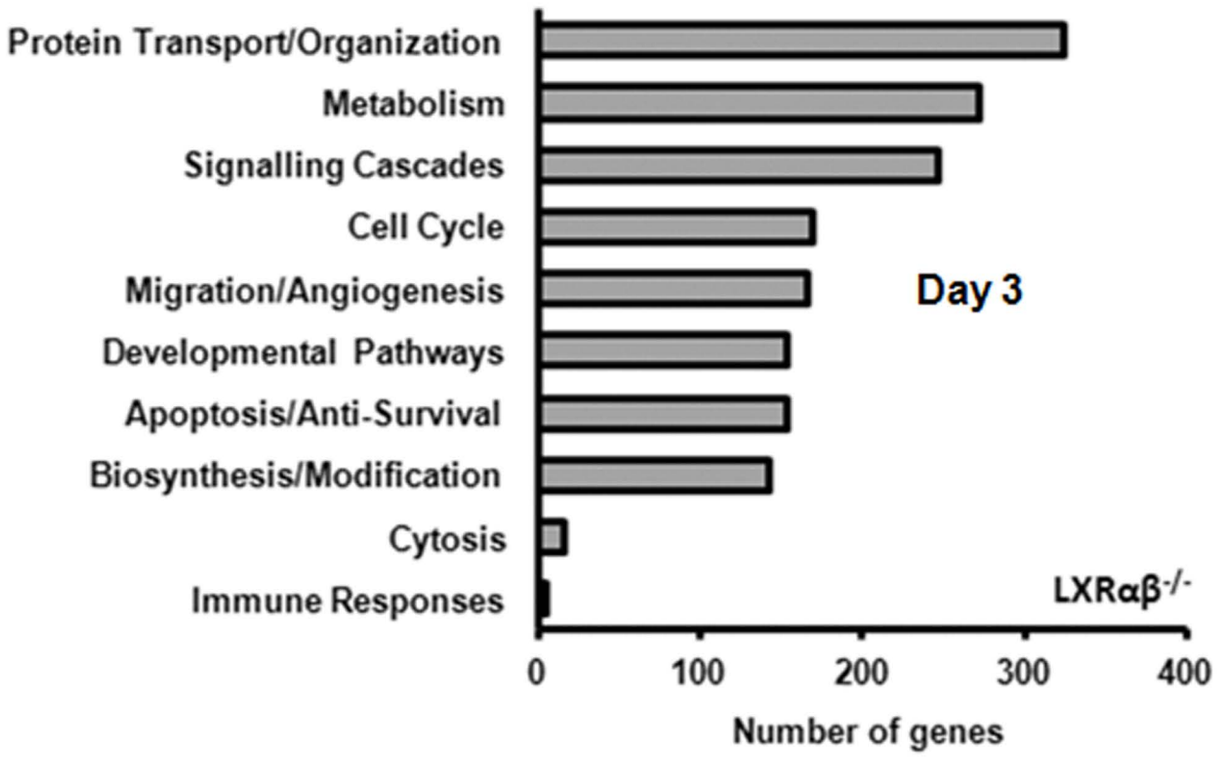
Protein Transport/Organization
Metabolism
Signalling Cascades
Cell Cycle
Migration/Angiogenesis
Developmental Pathways
Apoptosis/Anti-Survival
Biosynthesis/Modification
Cytosis
Immune Responses
Day 3
LXRαβ-/-
0
100
200
300
400
Number of genes

Freshly Isolated Murine Hepatic Stellate Cells (Day 0)

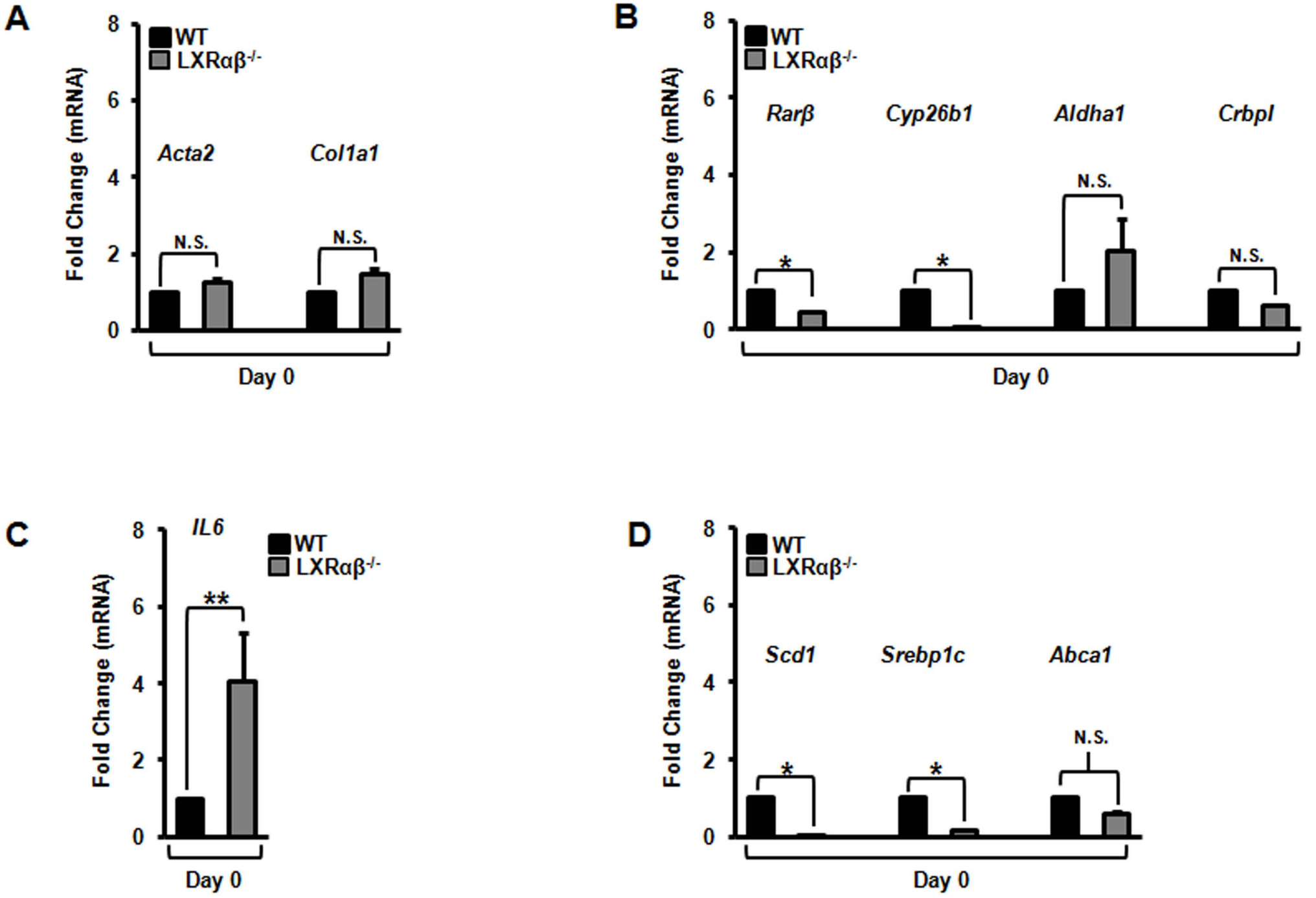

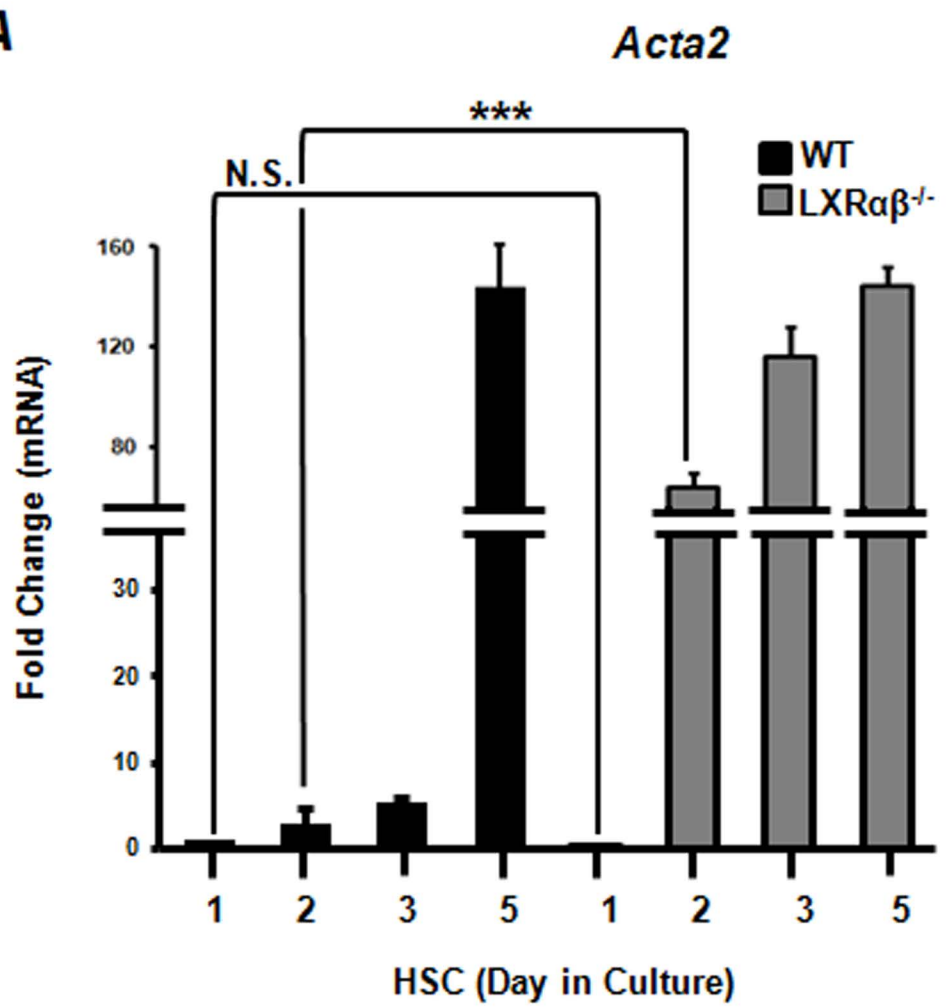
A
Acta2
***
N.S.
WT
LXRαβ-/-
Fold Change (mRNA)
160
120
80
30
20
10
0
1 2 3 5 1 2 3 5
HSC (Day in Culture)

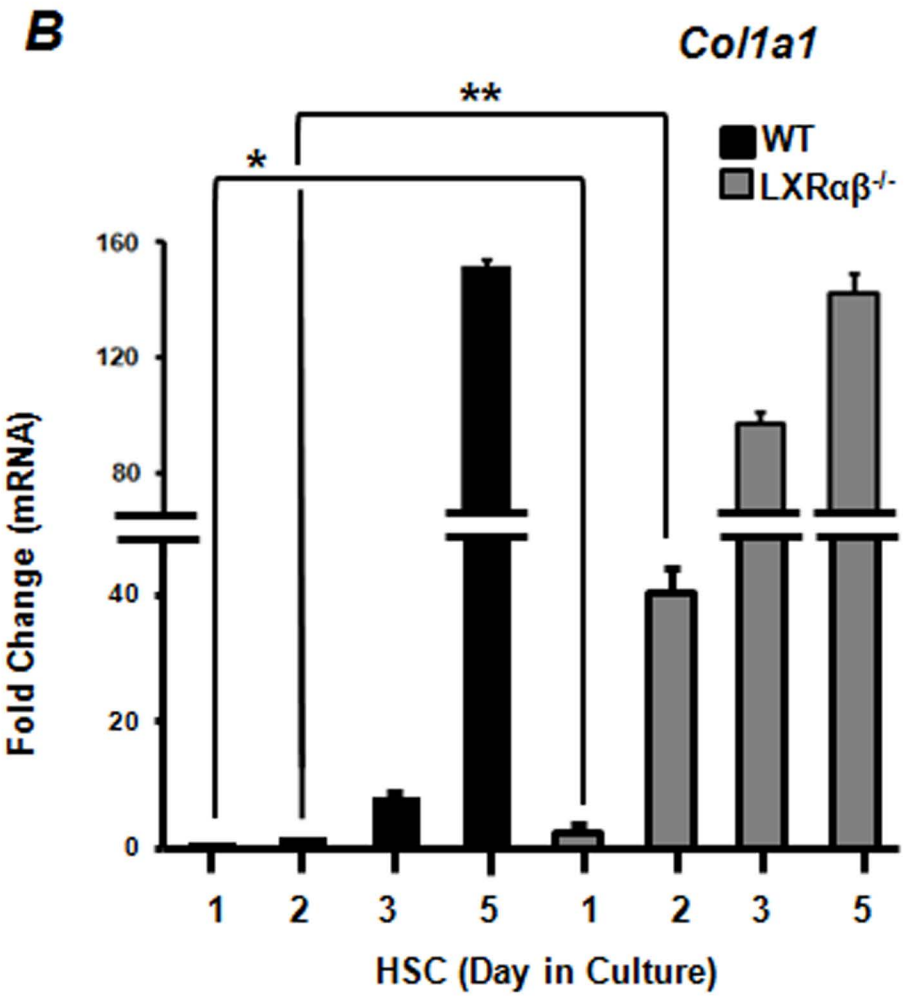
B
Col1a1
**
*
WT
LXRαβ-/-
Fold Change (mRNA)
160
120
80
40
20
0
1 2 3 5 1 2 3 5
HSC (Day in Culture)

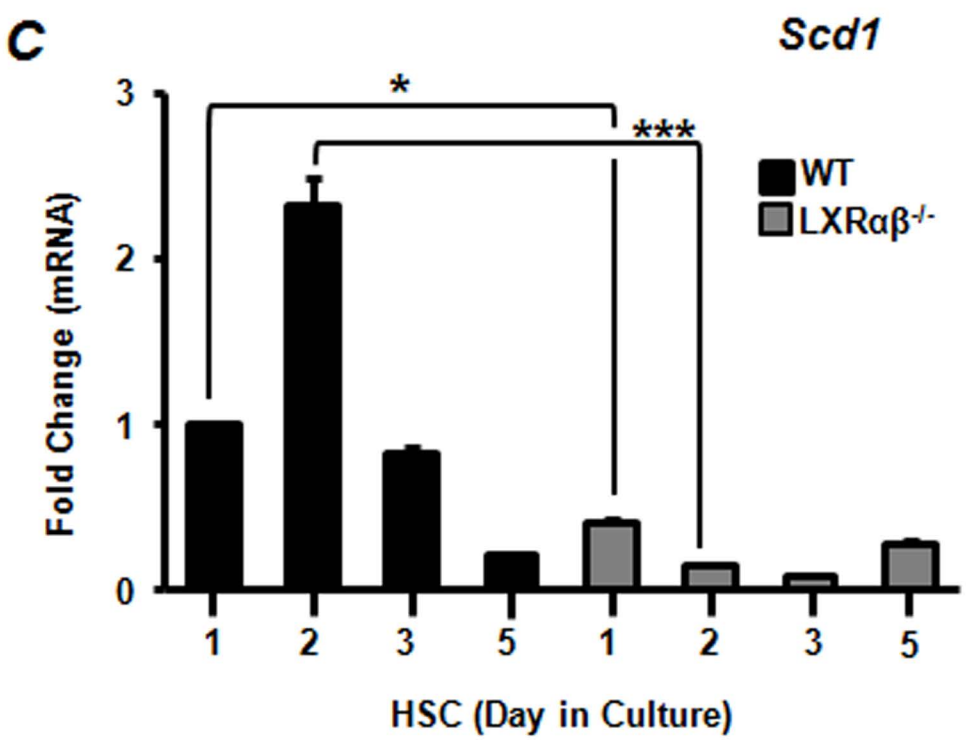
C
Scd1
*
***
WT
LXRαβ-/-
Fold Change (mRNA)
3
2
1
0
1 2 3 5 1 2 3 5
HSC (Day in Culture)

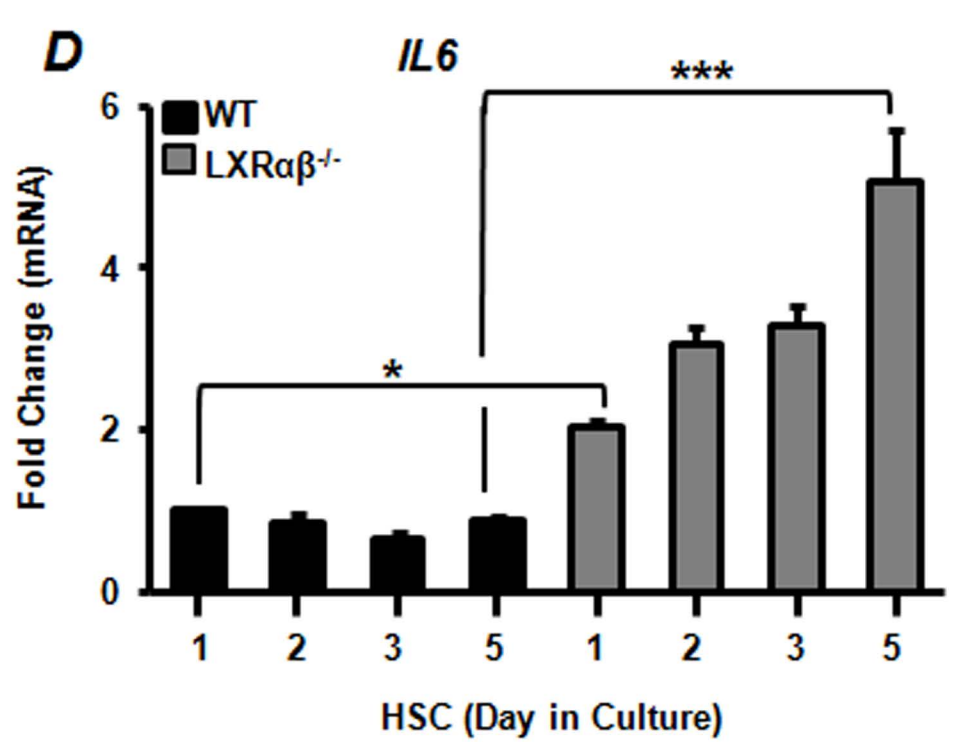
D
IL6
***
*
WT
LXRαβ-/-
Fold Change (mRNA)
6
4
2
0
1 2 3 5 1 2 3 5
HSC (Day in Culture)

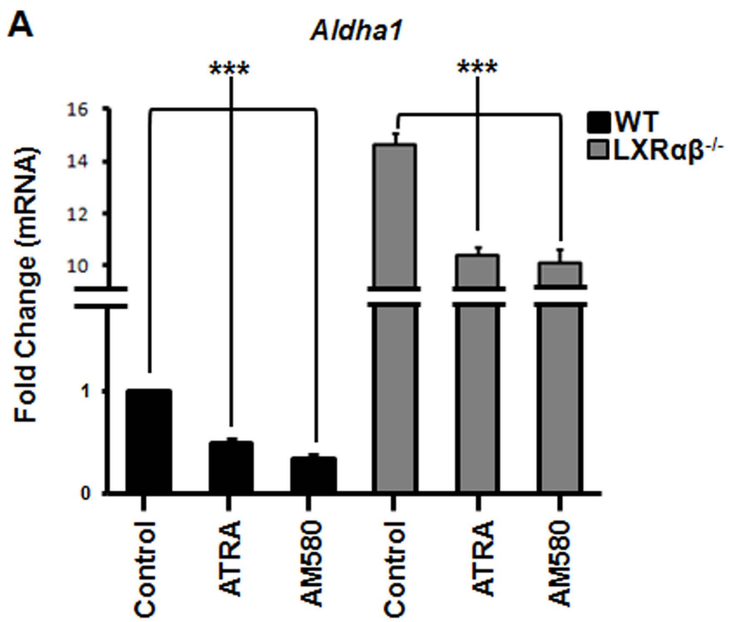
A
Aldha1
***
***
WT
LXRαβ-/-
Fold Change (mRNA)
16
14
12
10
1
0
Control
ATRA
AM580
Control
ATRA
AM580

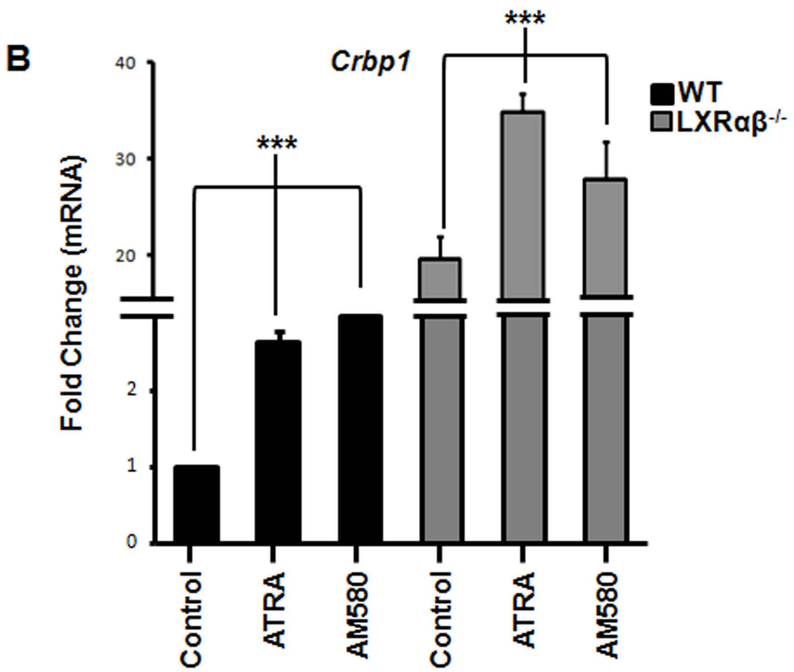
B
Crbp1
***
***
WT
LXRαβ-/-
Fold Change (mRNA)
40
30
20
2
1
0
Control
ATRA
AM580
Control
ATRA
AM580

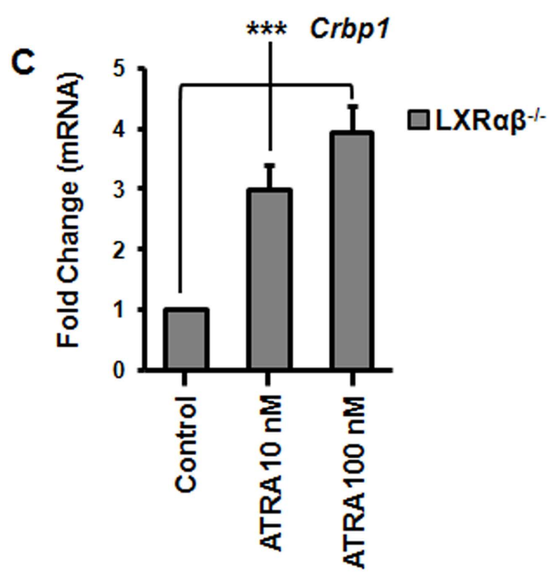
C
*** Crbp1
LXRαβ-/-
Fold Change (mRNA)
5
4
3
2
1
0
Control
ATRA 10 nM
ATRA 100 nM

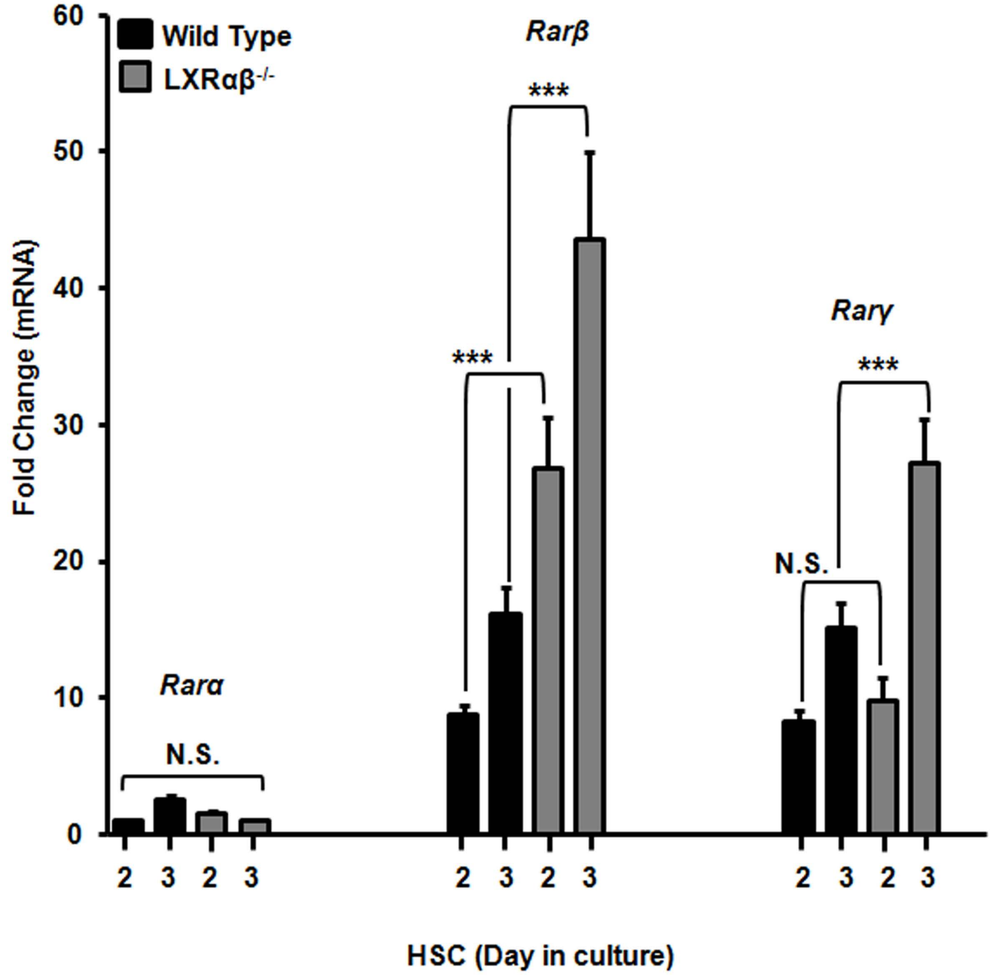
D
Wild Type
LXRαβ-/-
Rarβ
***
***
Rarγ
***
Rarα
N.S.
Fold Change (mRNA)
60
50
40
30
20
10
0
2 3 2 3
2 3 2 3
2 3 2 3
HSC (Day in culture)

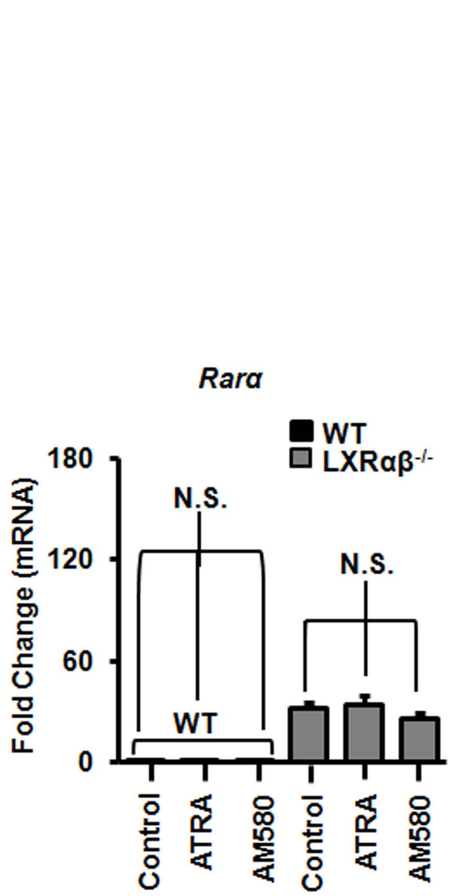
Rarα
WT
LXRαβ-/-
N.S.
N.S.
WT
Fold Change (mRNA)
180
120
60
0
Control
ATRA
AM580
Control
ATRA
AM580

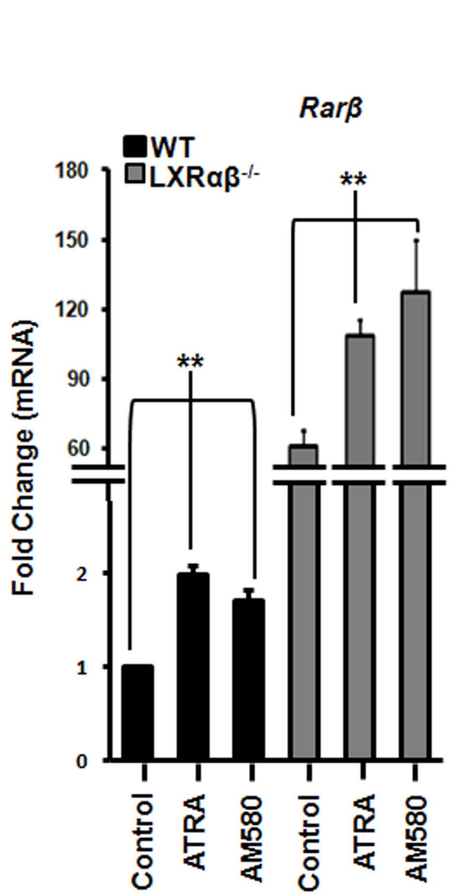
Rarβ
WT
LXRαβ-/-
**
**
Fold Change (mRNA)
180
150
120
90
60
2
1
0
Control
ATRA
AM580
Control
ATRA
AM580

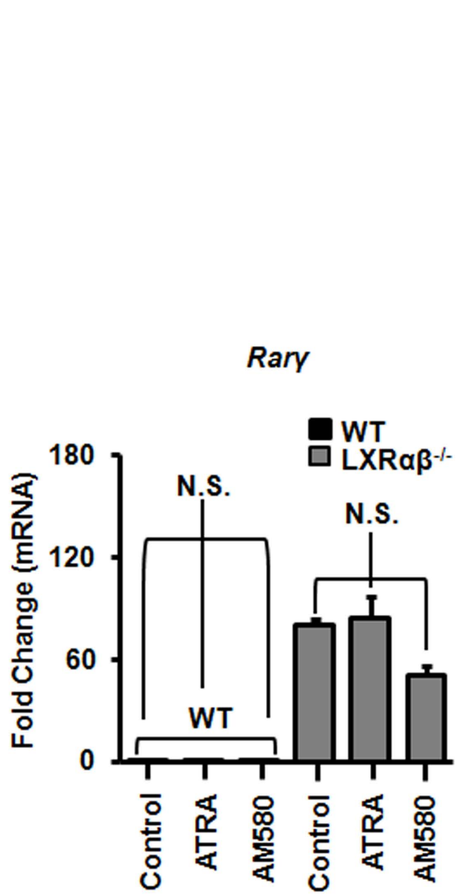
Rarγ
WT
LXRαβ-/-
N.S.
N.S.
WT
Fold Change (mRNA)
180
120
60
0
Control
ATRA
AM580
Control
ATRA
AM580

A
Plin1
Plin2
Plin3
Plin5
Relative Expression
WT HSC
LXRαβ-/- HSC
WT WAT
LXRαβ-/- WAT
10T
3T3
B
Plin2
Plin3
WT
LXRαβ-/-
Fold Change (mRNA)
N.S.
***
HSC (Day in Culture)
C
Plin2 Protein Band Intensity (Pixel)
Plin3 Protein Band Intensity (Pixel)
**
Day
Mem
Plin2
Plin3
Na+ K+ ATPase
Mem = Membrane
D
LXRαβ -/- Membrane
LXRαβ -/- Cytoplasm
Day 1
Day 3
LXRαβ -/- Cell Fractionation Controls
β-Actin
Cytoplasm
Membrane
GAPDH

A

Rab18

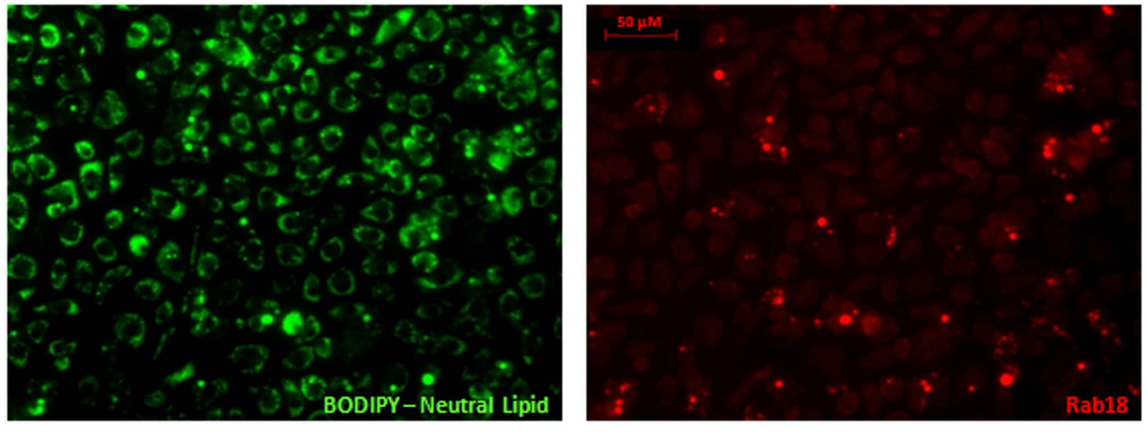

Plin3

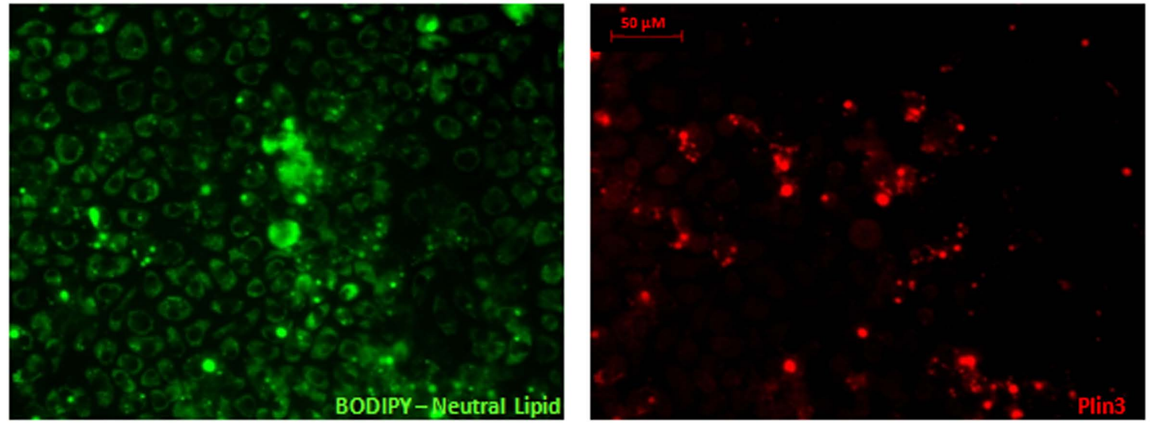

B

Plin3

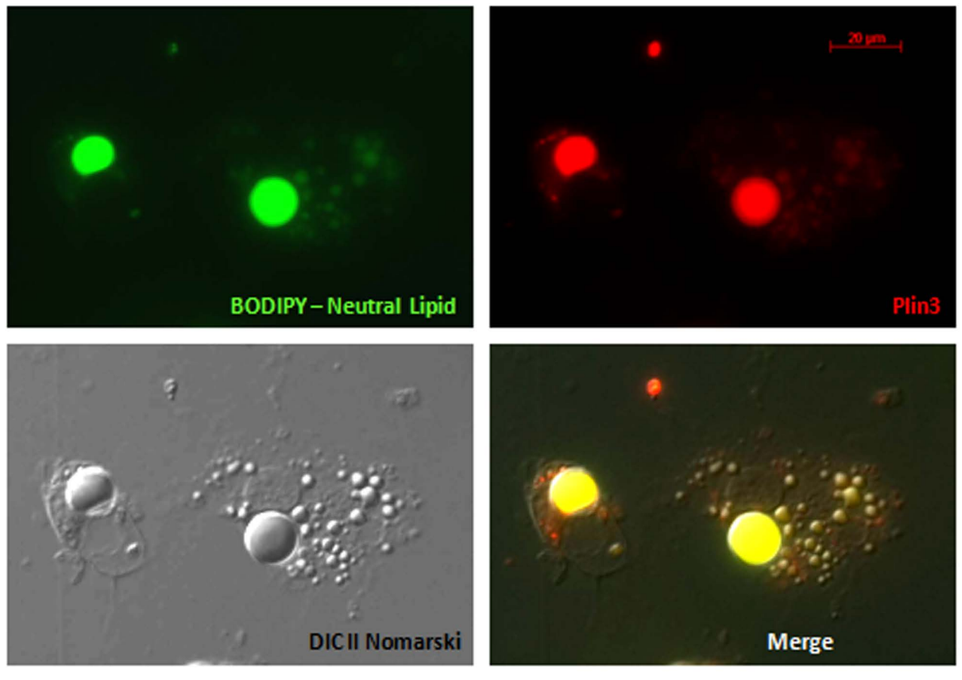

Plin2

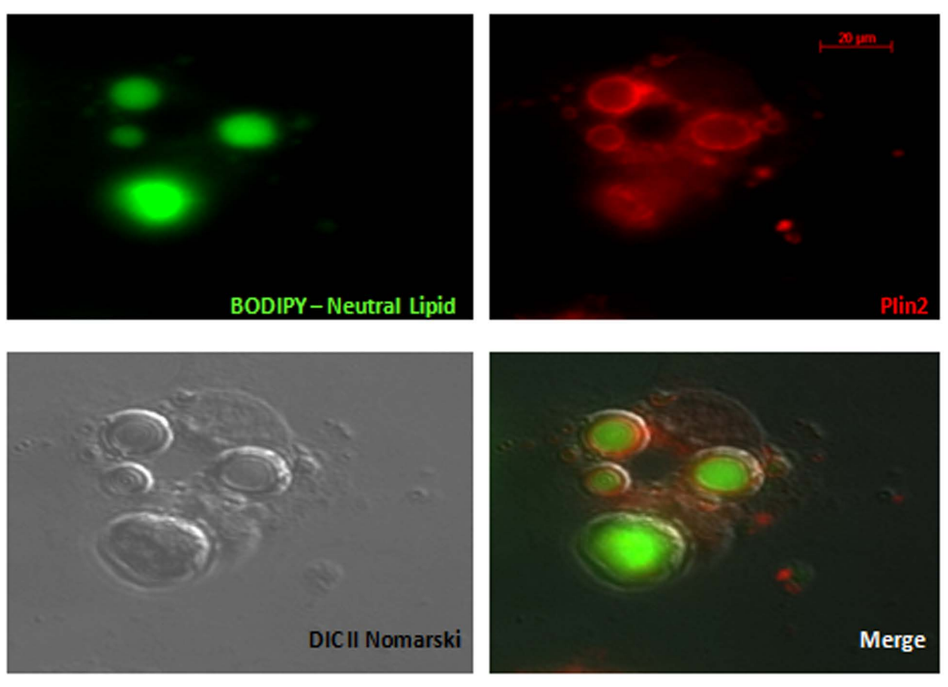

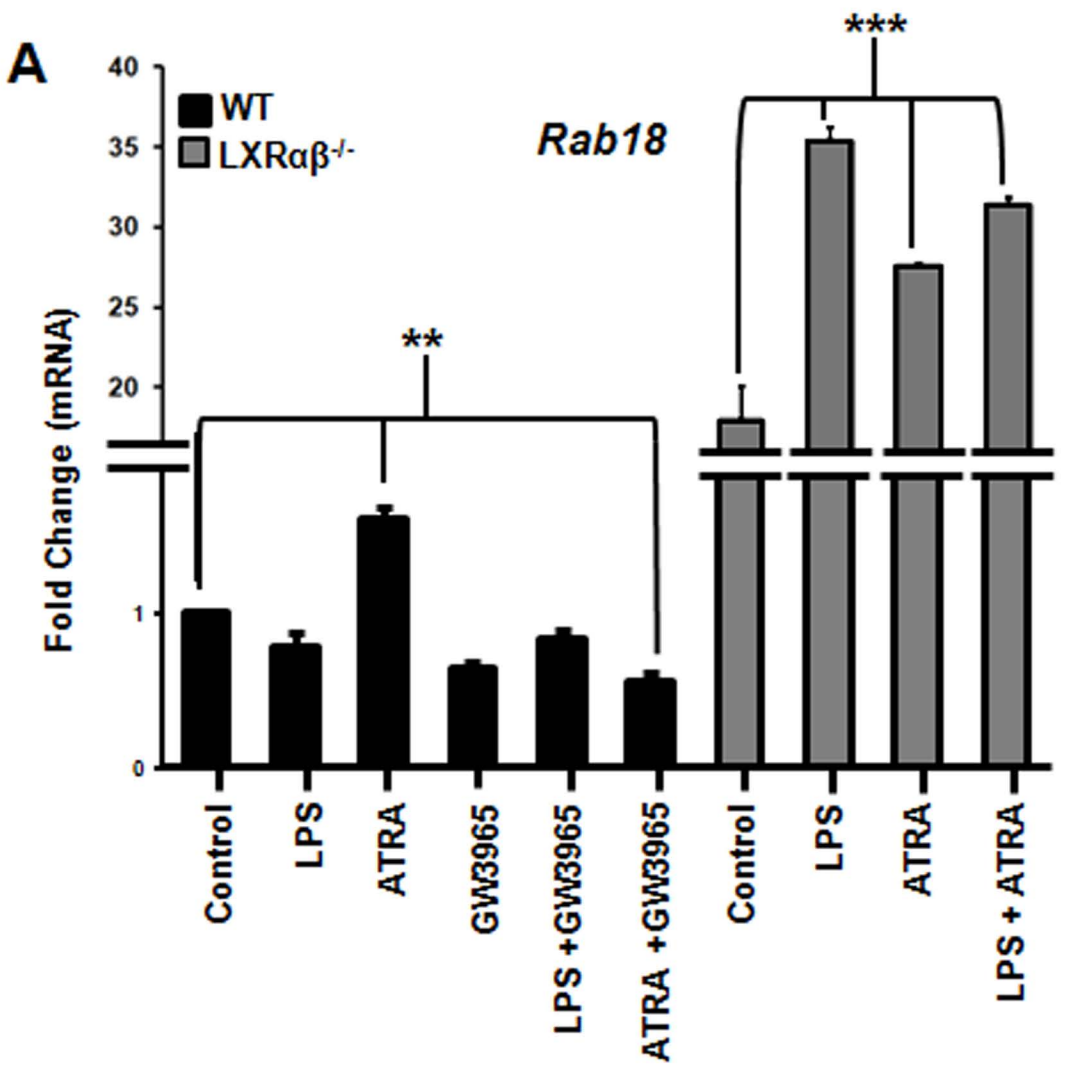
A
Rab18
WT
LXRαβ-/-
Fold Change (mRNA)
40
35
30
25
20
1
0
**
***
Control
LPS
ATRA
GW3965
LPS +GW3965
ATRA +GW3965
Control
LPS
ATRA
LPS + ATRA

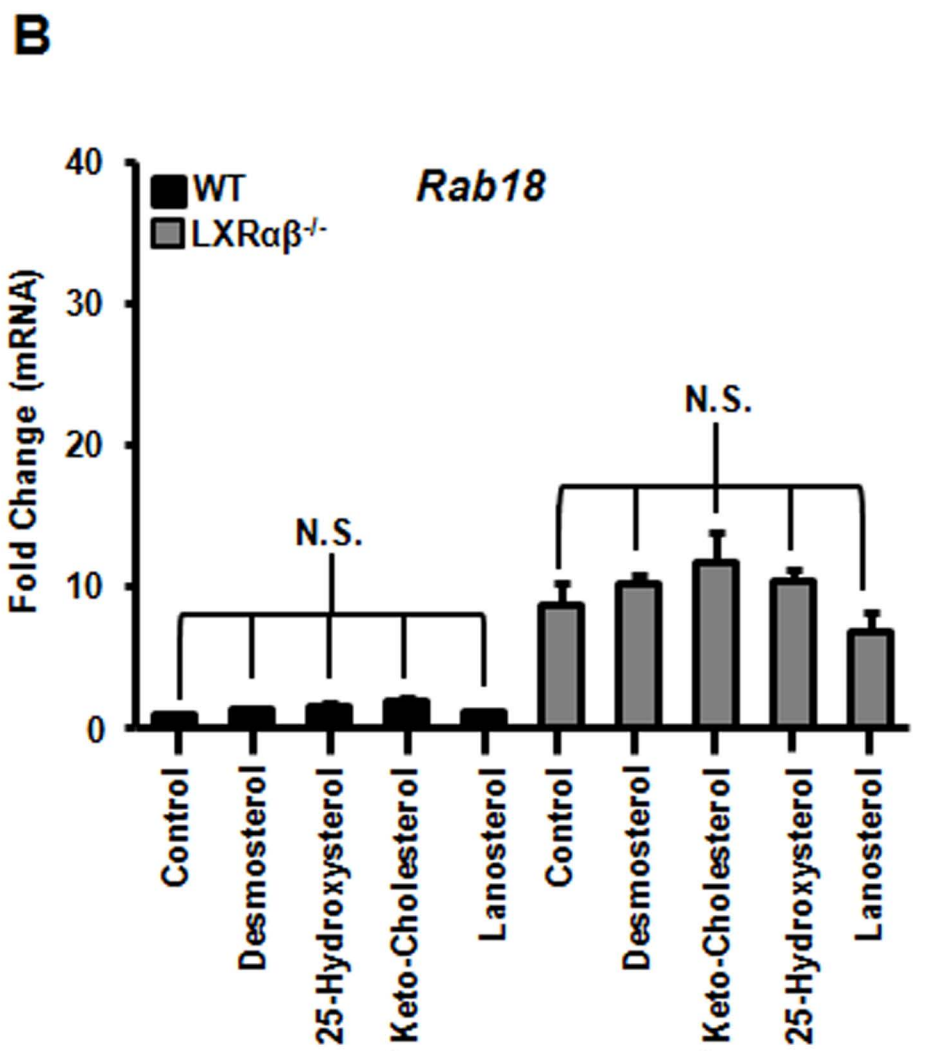
B
Rab18
WT
LXRαβ-/-
Fold Change (mRNA)
40
30
20
10
0
N.S.
N.S.
Control
Desmosterol
25-Hydroxysterol
Keto-Cholesterol
Lanosterol
Control
Desmosterol
Keto-Cholesterol
25-Hydroxysterol
Lanosterol

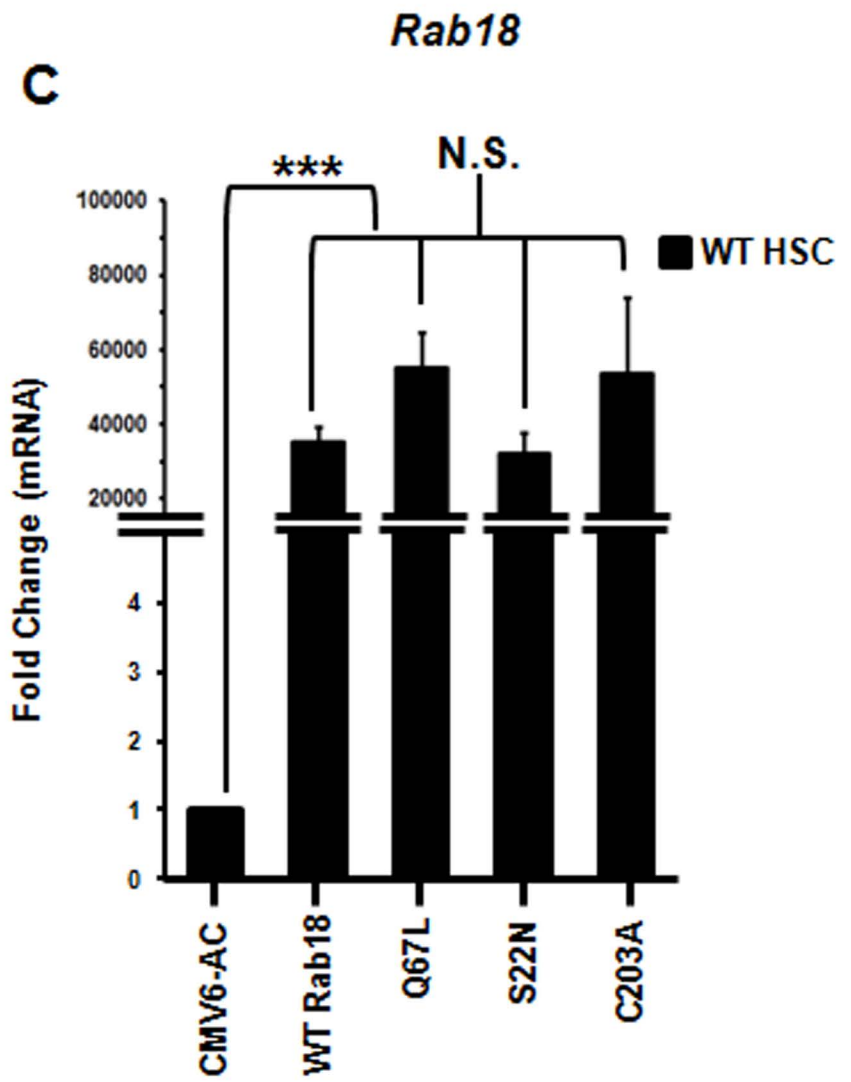
C
Rab18
WT HSC
Fold Change (mRNA)
100000
80000
60000
40000
20000
4
3
2
1
0
***
N.S.
CMV6-AC
WT Rab18
Q67L
S22N
C203A

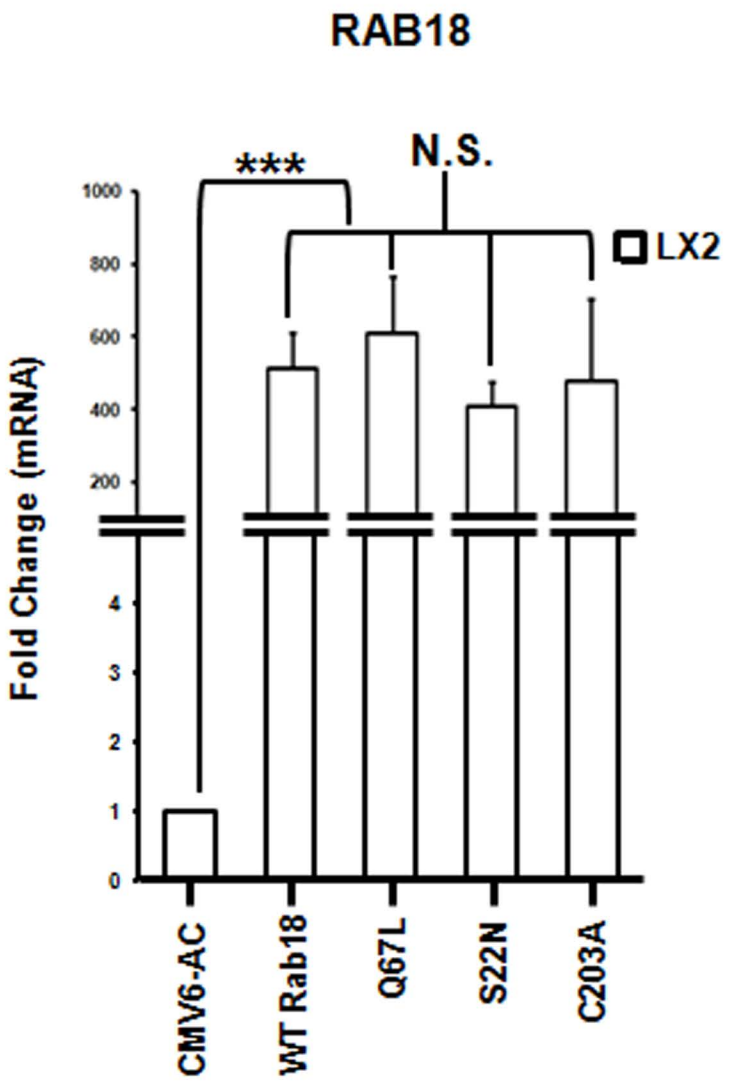
D
RAB18
LX2
Fold Change (mRNA)
1000
800
600
400
200
4
3
2
1
0
***
N.S.
CMV6-AC
WT Rab18
Q67L
S22N
C203A

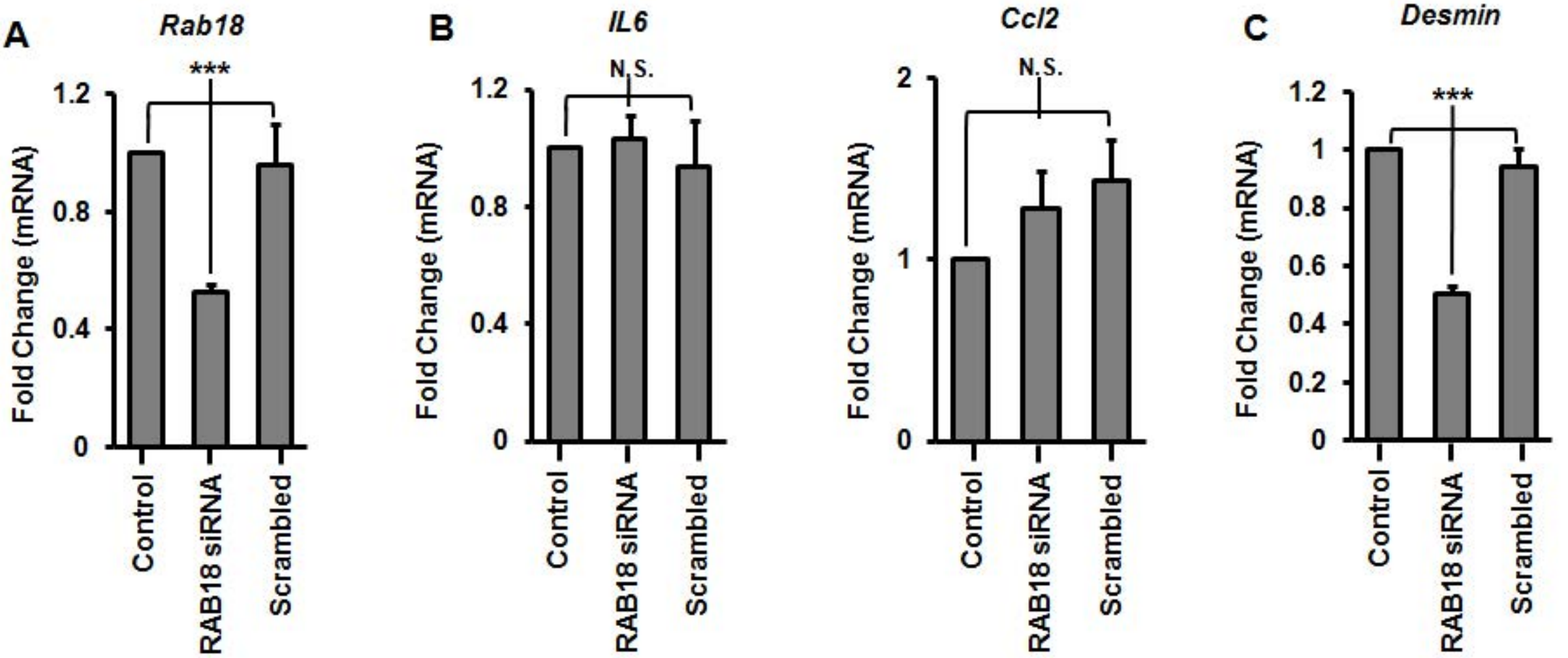
A
Rab18
***
Fold Change (mRNA)
1.2
0.8
0.4
0
Control
RAB18 siRNA
Scrambled
B
IL6
N.S.
Fold Change (mRNA)
1.2
0.8
0.4
0
Control
RAB18 siRNA
Scrambled
Ccl2
N.S.
Fold Change (mRNA)
2
1
0
Control
RAB18 siRNA
Scrambled
C
Desmin
***
Fold Change (mRNA)
1.2
1
0.8
0.6
0.4
0.2
0
Control
RAB18 siRNA
Scrambled
D
Timp1
***
Fold Change (mRNA)
1.2
1
0.8
0.6
0.4
0.2
0
Control
RAB18 siRNA
Scrambled
Timp2
***
Fold Change (mRNA)
1.2
1
0.8
0.6
0.4
0.2
0
Control
RAB18 siRNA
Scrambled
E
Pdgfr
***
Fold Change (mRNA)
1.2
1
0.8
0.6
0.4
0.2
0
Control
RAB18 siRNA
Scrambled
F
Mmp2
***
Fold Change (mRNA)
1.2
1
0.8
0.6
0.4
0.2
0
Control
RAB18 siRNA
Scrambled